Correlation of Swelling and Crosslinking Density with the Composition of the Reacting Mixture Employed in Radical Crosslinking Copolymerization

Isabel E. Pacios,[1] M. Jesús Molina,[1] M. Rosa Gómez-Antón,[2] Inés F. Piérola[1]

[1]*Departamento de Ciencias y Técnicas Fisicoquímicas, Facultad de Ciencias, Universidad a Distancia (UNED), 28040 Madrid, Spain*
[2]*Departamento de Química Aplicada a la Ingeniería, ETSI Industriales, Universidad a Distancia (UNED), 28040 Madrid, Spain*

ABSTRACT: This article reports the scaling laws relating the synthesis conditions with the crosslinking density (v_e) and swelling degree (S) of poly(N-vinylimidazole) hydrogels (PVI) prepared by radical crosslinking copolymerization in aqueous solution, with N,N'-methylene bisacrylamide (BA) as crosslinker. Multiple linear regression of v_e versus BA concentration ([BA]) and total comonomers concentration (C_T) in double log scale render the scaling law $v_e \sim C_T^{0.81} \times [BA]^{1.04}$ as comparable to that predicted by the model of polymer network with pendant vinyl groups ($v_e \sim C_T \times [BA]$), and showing inverse dependence on C_T to that expected, following from stoichiometry, for an ideal network ($v_e \sim 2[BA]/C_T$). S scales with v_e through a solvent-dependent exponent ranging from -0.46 to -0.54, only slightly over the value predicted by the Flory–Rehner theory (-0.6) or the blob's model by de Gennes (-0.5 to -0.8). Finally, the scaling law of S with the composition of the reacting mixture is also solvent-dependent and it seems to result not only from the dependence of v_e on C_T and [BA] but also from that of v_{2r}, the polymer volume fraction in the reference state, and χ, the polymer–solvent interaction parameter. Models used seem to overestimate the contribution of entanglements to the effective crosslinking density of PVI. © 2006 Wiley Periodicals, Inc. J Appl Polym Sci 103: 263–269, 2007

Key words: scaling; swelling; crosslinking; poly(N-vinylimidazole); hydrogel

INTRODUCTION

Hydrogels are physically or chemically crosslinked polymers, which have a wide range of applications and show numerous effects of scientific interest. It would be very useful to accurately establish the relationships between the properties of a crosslinked polymer (e.g., the equilibrium swelling degree, S) and the monomer and crosslinker concentrations in the reacting mixture, not only because it would allow preparation of samples with intended characteristics, but also because it would provide some understanding on the role played by network defects and heterogeneities in determining the properties of real polymer networks. This is the aim of this work, which will focus on polymer networks synthesized by radical crosslinking copolymerization and in particular on poly(N-vinylimidazole) hydrogels (PVI).[1,2]

The swelling equilibrium of many different gels depends inversely on the total comonomers concentration (C_T) and the crosslinker concentration (c_{xl}) employed in the polymerization feed mixture.[3–8] Theoretical support of these empirical relationships comes from scaling laws relating S and the average number of monomer units between two connected crosslinks,[9–13] N, and from less frequent laws relating N with the comonomers (C_T) and crosslinker (c_{xl}) concentrations in the feed.[3,6]

The simplest model of the dependence of N (N_{IN} for this model) on C_T and c_{xl} considers that for ideal polymer networks (IN), without defects, with knots functionality ϕ, is[10] $N_{IN} = 2C_T/\phi c_{xl}$. This ideal value is never achieved and the crosslinking efficiency measured by the ratio of N_{IN} and the experimental N, takes values below 1 because of network defects that involve crosslinker molecules and do not give place to elastically effective knots of the polymer network.[14,15] Dangling chains, intramolecular cyclizations, multifunctional knots formed by sequences of crosslinker or crosslinker molecules, which incorporate to the polymer network through only one of its vinyl groups, are common types of network defects that decrease the crosslinking efficiency. Entanglements, interchain hydrogen bonds, hydrophobic interactions or other physical interactions contribute positively to the experimentally determined effective crosslinking density, which is the sum of contributions

of permanent or covalent crosslinks, network defects, and specific topologies of the system. Some of these types of contributions were considered in the developing of polymer network theoretical models.

The model by Bromberg et al.[3] considers polymer networks with only one type of defect, pendant unreacted vinyl groups (PNPV), and puts forward that the average number of monomer units in chains between crosslinks (N_{PV} for this model) depends on ($c_{xl} \times C_T)^{-1}$. This statistical model treats polymerization as a set of random walks beginning from the initiator and progressing randomly through the bifunctional monomer and crosslinker surrounding it. Several basic assumptions of the model do not significantly limit its applicability; for example, the concentration of initiator must be much smaller than that of the product $c_{xl} \times C_T^2$, which is a common practice. Other simplifying assumptions such as the equal reactivity of the bifunctional monomer and the first reacting vinyl of crosslinker or that of pendant vinyl, regardless of their environment, may be more important and have been discussed.[16] It is remarkable that the model of ideal network does also assume equal reactivity of vinyl groups, the only difference is that the PNPV model considers that given the Gaussian nature of random walks, the path length after g steps is $g^{1/2}$ and since the polymer concentration in the formed network, $g/g^{3/2}$, is proportional to C_T, g scales with C_T^{-2} in such way that N_{PV}, estimated as the ratio of g and the probability to meet a pendant vinyl group on another chain after g steps, $p = c_{xl}/C_T$, scales with ($c_{xl} \times C_T)^{-1}$. However, in an ideal network each crosslinker molecule becomes a knot and N_{IN} reflects the total amount of comonomers per crosslinker molecule in the feed. The important consequence of such difference is that N_{PV} depends on C_T^{-1} while N_{IN} depends on C_T^{+1}.

Several other theoretical studies take into account the influence of feed concentrations on the formation of entanglements and the contribution of entanglements to the effective crosslinking density and equilibrium swelling.[6,11–13] Classical theories of rubber elasticity assume[10] that entanglements simply restrict the fluctuations of crosslinks but currently, in the light of tube models,[17] it is admitted that entanglements introduce topological constraints acting as effective crosslinks and reinforcing the role of permanent or chemical crosslinks. The model proposed by Furukawa[6] for gels prepared with concentrated feeds (Gel II type) is based in the de Gennes' blob model[9] ($S \sim N^{3v-1}$ with $v = 3/5$ in good solvent and $v = 1/2$ in theta solvent) combined with the model by Oblukhov et al.[12] ($S \sim C_T^{-b}$ with $b = 1$ in good solvent and $b = 3/4$ in theta solvent) to take into account topological entanglements not treated in the blob model. After this model[6] of polymer network with entanglements, in the notation of this work, $S \sim N_{IN}^{0.25} \times C_T^{-1.17} = c_{xl}^{-0.25} \times C_T^{-0.92}$. A more complex model is given in the same reference to

explain jointly the swelling behavior of gels prepared in concentrated (Gel II) and in dilute feeds close to those giving place to sol phases (Gel I), but it won't be considered because it is out of the scope of this work.

The effect of entanglements on the equilibrium swelling was also investigated using Monte Carlo simulations.[11] More entanglements entail less swelling in such a way that S scales with $C_T^{-\xi}$ and the scaling exponent ξ increases as the crosslinker content decreases, thus reflecting the degree of entanglement. $\xi = 1$ is the maximum value[12] and corresponds to entanglement dominated systems with chains between permanent crosslinks much larger than the chain entanglement size of that particular system. The role of entanglements in diminishing swelling depends strongly on the proximity of the time of polymerization at which the reaction was stopped, to the gel point.[13]

The objective of this work is to ascertain the validity of the model of PNPV. The idea that the expected crosslinking density must be estimated as that of the ideal polymer network is deeply discussed in the literature of the field. Nevertheless, the ideal network model fails both qualitative and quantitatively whereas the PNPV model, which is as the model of ideal network has no fitting parameter,[3,7,8] may be a better approach. We have chosen for this study PVI hydrogels because of their remarkable properties: they are quite effective in uptaking metal cations or in regulating the pH of aqueous media without dissolving.[1,2] Besides, they are neutral or ionic, depending on the swelling medium[7,18,19] thus making them very useful in studying typical hydrogel effects such as thermo- or pH-responsiveness.[18–21] From the commercial point of view, they are also important in the construction of enzyme electrodes for the determination of sugars[22] or as supports for solid-phase extraction.[23]

EXPERIMENTAL

Poly(N-vinylimidazole) hydrogel samples (PVI) were synthesized by radical crosslinking copolymerization of N-vinylimidazole (VI) and N,N'-methylene-bisacrylamide (BA) in aqueous solution, with 2,2'-azobis(isobutyronitrile) (AIBN), $6 \times 10^{-3}M$ as initiator. N-vinylimidazole (Aldrich) was distilled under reduced pressure, just prior to use. Water was distilled and deionized by a Milli-Q system from Millipore; AIBN (Fluka) and BA (Aldrich) were used as received. The concentration of VI and BA ([VI] and [BA]) was different in the feed of each sample (see Table I) with total comonomer concentrations, C_T, ranging from 1.8 to 6.2M and [BA] from 0.03 to 0.23M. The aqueous solution of VI, BA, and AIBN was sonicated at 60°C for 10 min and then it was immersed in a bath at 90°C for 2 h. The degree of conversion was within 85 ± 10%. After polymerization, the hydrogels were taken out of molds, cut as disk-like pellets of about 1 cm diameter and 1 mm

TABLE I
Glass Transition Temperature and Concentrations
of Crosslinker and Bifunctional Comonomer Employed
in the Synthesis of PVI Samples

Sample code	[VI] (mol/L)	[BA] (mol/L)	$C_T \times$ [BA] (mol/L)^2	T_g (°C)
PVI20(2)	2.08	0.029	0.061	187.3
PVI20(3)	2.06	0.041	0.086	186.3
PVI20(4)	2.03	0.055	0.115	187.4
PVI20(6)	1.99	0.084	0.174	186.4
PVI20(10)	1.89	0.146	0.297	188.0
PVI20(15)	1.75	0.230	0.455	188.9
PVI40(2)	4.16	0.054	0.228	186.7
PVI40(3)	4.12	0.080	0.336	–
PVI40(4)	4.07	0.109	0.456	–
PVI40(6)	3.98	0.166	0.688	184.8
PVI30(2)	3.12	0.040	0.126	183.0
PVI50(2)	5.20	0.067	0.353	188.2
PVI60(2)	6.24	0.080	0.506	187.3
PVI30(4)	3.06	0.079	0.249	187.2
PVI50(4)	5.09	0.136	0.711	186.4

thickness and washed repeatedly with Milli-Q water for about one month; water was replaced frequently and spectrophotometrically analyzed to detect the end of the extraction of soluble material, in particular, of residual VI. Clean hydrogels were dried in oven at 80°C for 24 h.

Swelling measurements in methanol, ethanol, and deionized water were performed gravimetrically by immersing dry samples in the swelling solvent for about one week. From time to time, samples were removed from the bath, blotted with tissue paper to dry the surface fluid and weighed. Once they reached a constant weight, (m_h), the equilibrium swelling degree, S, was determined as the ratio of the weight of swelling solvent ($m_h - m_o$), to the weight of the dry gel (m_o)

$$S = (m_h - m_o)/m_o \qquad (1)$$

The polymer volume fraction in the equilibrium swollen state, v_2, and the swelling degree, S, are related through xerogel (ρ_2) and swelling solvent (ρ_1) densities:

$$v_2 = (1 + \rho_2 S/\rho_1)^{-1} \qquad (2)$$

Xerogel density was pycnometrically determined with acetone as nonsolvent of PVI.[24] An important parameter in swelling analysis is v_{2r}, the polymer volume fraction in the relaxed network state, i.e., when the crosslinkages were introduced. It was measured just after polymerization and determined with eqs. (1) and (2). The yield of the polymerization is

$$\beta = 100 v_{2r}/(C_T \times V_2) \qquad (3)$$

with V_2 being the molar volume of the polymer repeating unit in L/mol.

The thermal analysis was carried out by differential scanning calorimetry (DSC) in a Mettler TC11 instrument provided with a DSC 30 oven and a subambient cooling unit. Two runs were performed with each specimen (5–10 mg), in nitrogen atmosphere, using an empty aluminum cell as a reference. Both runs were scanned at 10°C/min and were extended to 300°C, a temperature well below the beginning of thermal instability of PVI xerogels: loss weight at 300°C is below 4% in any sample studied here. Only second run results were considered.

Scanning electron microscopy (SEM) measurements were carried out in a JEOL JSM 6400 electron microscope. Solid specimens were prepared by critical point drying of samples swollen in supercritical CO_2 using a Balzers SCD 030 critical point dryer. Swelling in supercritical CO_2 was preceded by slow and progressive exchange of swelling water by acetone and later of acetone by supercritical CO_2. In all cases, solid specimens were coated with gold by means of a Balzers SCD 004 sputter-coater. Surface and bulk structures were observed. Inner parts of the specimens were revealed by simply cutting them with a bistoury or by cryogenic fracture.

RESULTS AND DISCUSSION

PVI samples were characterized by measuring their glass transition temperatures (T_g) and their microstructure. Table I summarizes the T_g observed for the samples studied here. It is in all cases above the T_g of the uncrosslinked PVI (182°C) because permanent crosslinks limit chain mobility causing an increment of T_g. Nevertheless, the increment of T_g with respect to that of the uncrosslinked polymer does not increase proportionally to the crosslinking density measured by [BA] $\times C_T$ (see below) and remains within a short range (183–189°C). The reason for that behavior is that samples synthesized with high [BA] form densely crosslinked domains that should contribute to the observed glass transition with large T_g but in fact their contribution disappears in the base line, i.e., they are opaque to DSC.[24]

Figure 1 shows a representative SEM micrograph of a PVI solid sample, retaining the porous structure that it had in the swollen state, due to the drying method employed. Thus, it seems that the polymer matrix forms a fibrillar network with mesh size of about 0.3 μm, as observed for other hydrogels.[25,26] In the swollen state, solvent fills the micropores and penetrates the polymer matrix, and those two contributions yield a given swelling degree inversely proportional to the polymer crosslinking density.

For neutral hydrogels swollen at equilibrium, the polymer–solvent mixing contribution to the osmotic swelling pressure (Π_{mix}) balance with the elastic contribution (Π_{el}).[10] The Flory–Rehner equation,[10] modified
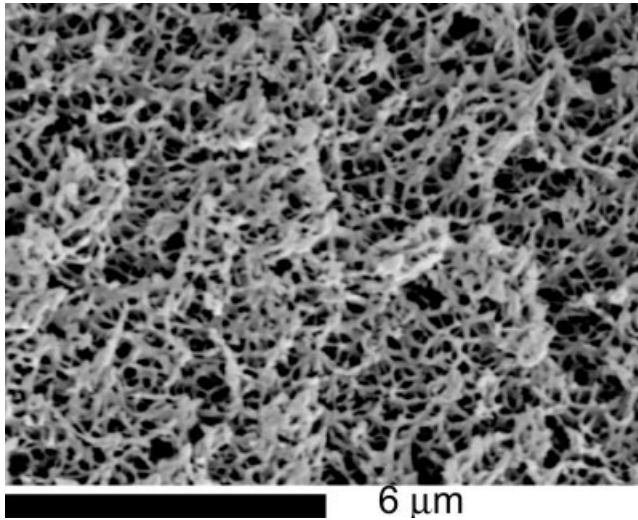
Figure 1 Micrograph of sample PVI20(2) prepared for SEM by critical point drying from its swollen state in deionized water.

to take into account v_{2r}, the polymer volume fraction just after polymerization,[27] expresses such balance ($\Pi_{mix} = -\Pi_{el}$) and relates v_2 with v_e, the effective crosslinking density:

$$\ln(1 - v_2) + v_2 + \chi v_2^2 + V_1 v_e(v_{2r}^{2/3} v_2^{1/3} - 2v_2/\phi) = 0 \quad (4)$$

where V_1 represents the solvent molar volume and ϕ knots functionality, with $\phi = 4$ for BA. To determine v_e of PVI hydrogels, we employed water as swelling solvent, with the polymer–solvent interaction parameter (χ) previously determined[7] as a linear function of v_2.

The most extended way of estimating the crosslinking density from the composition of the polymerization mixture is based in the ideal network model with

$$v_c(IN) = (\rho_2/M_o) \times [BA]/C_T \quad (5)$$

where $v_e(IN)$ represents the crosslinking density values predicted by the ideal network model and M_o represents the molecular weight of the repeating unit. The plot of v_e values obtained with eq. (4) versus $[BA]/C_T$, is an unshaped cloud of points showing no correlation. It evidences that the ideal network model is not feasible. Contrarily, Figure 2 shows a good linear correlation of v_e with $[BA] \times C_T$. That points to a good feasibility of the PNPV model[3] after which, samples synthesized with the same $C_T \times [BA]$ are expected to have the same number of bonds in chains between adjacent crosslinks

$$N_{PV} = 1/2a^6 C_T [BA] \quad (6)$$

(with a^6 equal to 0.0116, the product of BA and VI molar volumes expressed in L/mol)[24] and therefore the same crosslinking density

$$v_e(PV) = \rho_2/M_o N_{PV} \quad (7)$$

where $v_e(PV)$ represents the crosslinking density values predicted by the PNPV model.

In the following text, the dependence of v_e and S on [BA] and C_T as much as the dependence of S on v_e, are more deeply analyzed.

Scaling laws for crosslinking density–feed composition

Figure 2 shows how the experimental crosslinking density of PVI samples is well represented by a linear
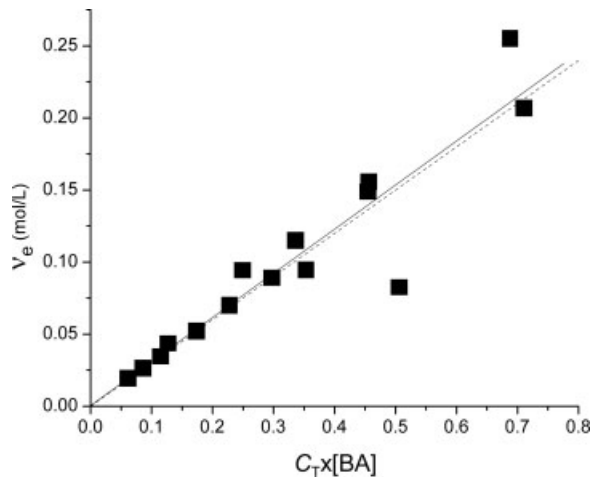

Figure 2 Crosslinking density of PVI determined from swelling measurements in deionized water (filled black points), crosslinking density calculated with the model of PNPV (dashed line, $v_e(PV) = 0.302C_T \times [BA]$ in mol/L) and linear fit of filled point results (solid line, slope 0.31 ± 0.06 and correlation coefficient 0.93).
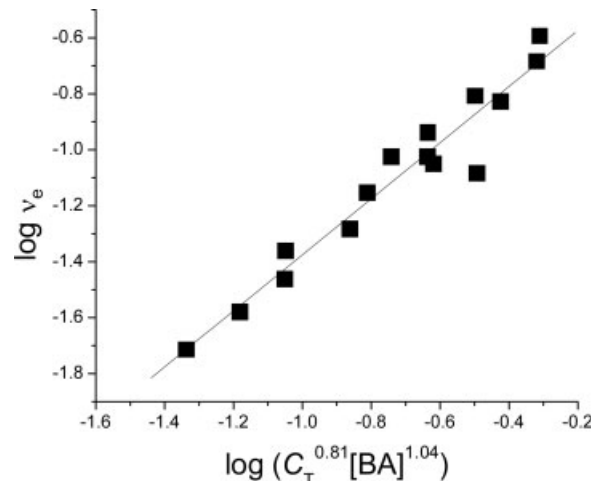

Figure 3 Scaling plot of the crosslinking density of PVI. The solid line corresponds to the linear fit with slope 1.00 ± 0.07 and correlation coefficient 0.97.

TABLE II
Scaling Laws of Swelling and Crosslinking Density

Crosslinking–feed	Swelling–crosslinking	Swelling–feed	
$\nu_e \sim 2c_{xl}/C_T$	$S \sim \nu_e^{-0.6} \times (1/2-\chi)^{0.6}$ (Ref. 10)	$S \sim C_T^{+0.6} \times c_{xl}^{-0.6}$	Model of ideal polymer network
	$S \sim \nu_e^{-(3v-1)}$	$S \sim C_T^{-0.92} \times c_{xl}^{-0.25}$ (Ref. 6)	Model of ideal polymer network with entanglements
	$0.5 < (3v-1) < 0.8$ (Ref. 9)		
$\nu_e \sim C_T \times c_{xl}$ (Ref. 3)	$S \sim \nu_e^{-0.6}$	$S \sim C_T^{-0.6} \times c_{xl}^{-0.6}$ (Ref. 3)	Model of PNPV
$\nu_e \sim C_T^{0.81} \times [BA]^{1.04}$	$S \sim \nu_e^{-0.54}$	$S \sim C_T^{-0.29} \times [BA]^{-0.67}$	This work, PVI–methanol
	$S \sim \nu_e^{-0.46}$	$S \sim C_T^{-0.34} \times [BA]^{-0.55}$	This work, PVI–ethanol
	$S \sim \nu_e^{-0.48}$	$S \sim C_T^{-0.67} \times [BA]^{-0.38}$	This work, PVI–water

function of $C_T \times [BA]$, as predicted by the PNPV model. In fact, the linear regression fit of ν_e experimental values and the line of calculated $\nu_e(PV)$ values do practically overimpose.

Multiple linear regression (MATLAB) of log ν_e versus log C_T and log [BA] solves for coefficients a_1 and a_2 in the expression log $\nu_e = a_0 + a_1$ log [BA] + a_2 log C_T providing $a_1 = 1.04$ and $a_2 = 0.81$. Hence, ν_e scales with $C_T^{0.81} \times [BA]^{1.04}$ better than with $C_T \times [BA]$ and this result is not in contradiction with Figure 2 since ν_e scales acceptably with $C_T \times [BA]$ but the linear correlation improves in the scaling plot versus $C_T^{0.81} \times [BA]^{1.04}$ shown in Figure 3, with respect to Figure 2.

This result is surprising; it would be easy to understand a scaling exponent of C_T larger than 1 because the model does not take into account entanglements and it is usually admitted that their contribution to the effective crosslinking density increases with C_T.[6,11] It would also be easy to admit an scaling exponent of [BA] smaller than 1 because the model does not include network defects other than pendant vinyl groups and the other type of defects decrease the contribution of [BA] to the formation of permanent crosslinks. But the physical meaning of a scaling exponent of C_T below 1 and smaller than the exponent of [BA], although not too different, is not clear. It may only be concluded that, in the frame of the PNPV model, the slight departure of the scaling exponent of C_T suggests that other type of defects and topologies, involving VI rather than BA, decreases slightly the contribution of C_T to the effective crosslinking density.

Scaling laws for swelling–crosslinking density

Table II summarizes theoretical and experimental scaling laws for swelling. The swelling degree, S, scales with $\nu_e^{-0.48 \pm 0.05}$ in deionized water, with $\nu_e^{-0.46 \pm 0.03}$ in ethanol, and with $\nu_e^{-0.54 \pm 0.05}$ in methanol. These exponents are solvent dependent and slightly different of that predicted by Flory,[10] but, as shown in Figure 4, the dispersion of points is not incompatible with the theoretical scaling law $S \sim \nu_e^{-0.60}$, which was experimentally observed for some other polymer networks.[5,28,29]

In Flory's treatment, the factor $(1/2-\chi)^{0.6}$ represents excluded volume effects in swelling (see Table II), taking χ from thermodynamic measurements on dilute solutions of the linear polymer analog.[10] Currently, it is admitted[30] that for polymer networks χ depends linearly on polymer concentration in the swollen network ($\chi = \chi_1 + \chi_2 v_2$) and thus, excluded volume effects would represent a solvent-dependent correction of the scaling law $S \sim \nu_e^{-0.60}$. In terms of the blob's model by de Gennes,[9] S scales with ν_e through a solvent-dependent exponent, which ranges (Table II) from -0.5 for theta solvents to -0.8 for good solvents. Hence, predictions of this model are also slightly different of the experimental exponents found for PVI. The value of χ_1 which represents the value of χ extrapolated to polymer dilute solutions ($v_2 = 0$) is about 0.5 for water and ethanol ($\chi_1 = 0.50$ for PVI-water and $\chi_1 = 0.49$ for PVI–ethanol) and therefore those two solvents could be considered as theta systems whereas $\chi_1 = 0.47$ for methanol, which corresponds to a slightly better solvent. In accordance with this fact, the exponent for methanol increases in regard to water and ethanol.

On the other hand, the polymer volume fraction, v_2, scales with ν_e through scaling laws slightly different than for S: $v_2 \sim \nu_e^{-0.41 \pm 0.04}$ in deionized water, $v_2 \sim \nu_e^{-0.40 \pm 0.03}$ in ethanol and $v_2 \sim \nu_e^{-0.48 \pm 0.04}$ in methanol. In theoretical treatments,[9,10] for simplicity, v_2 is assumed to be proportional to S^{-1} and therefore, the same scaling rules are expected both for v_2 and S^{-1}. Nevertheless, a slight difference of the absolute value of exponents for S and v_2 is experimentally observed. The reason for that discrepancy is that S is not larger than 10, the typical S value for neutral hydrogels, and in such conditions 1 is not negligible with respect to $\rho_2 S/\rho_1$ in eq. (2) and v_2 is not exactly equal to $(\rho_2 S/\rho_1)^{-1}$, i.e., v_2 is not proportional to S^{-1}. S is larger than 10 only for ionic hydrogels, but here we consider only scaling laws for S values of neutral hydrogels.

Scaling laws for swelling–feed composition

Table II summarizes the scaling laws relating S with C_T and [BA] for PVI in the three solvents considered here, obtained through multiple linear regression of the experimental results. Figure 5 visualizes the goodness of such fits in a bidimensional plot.
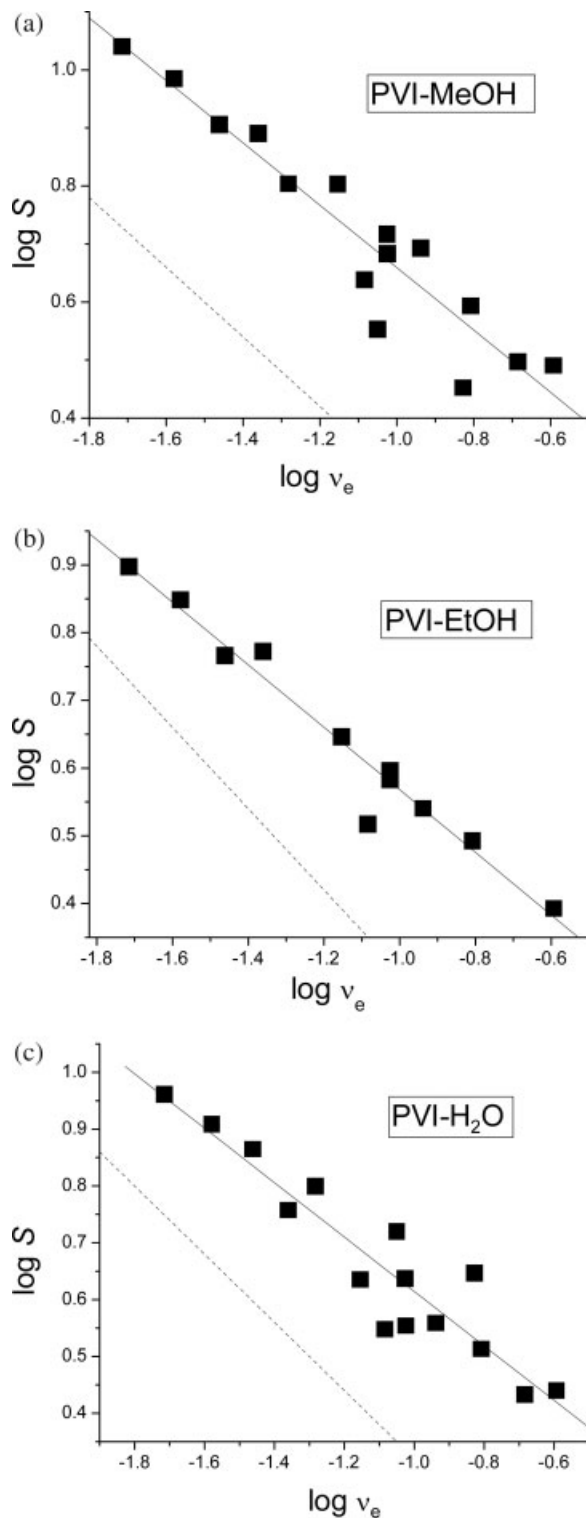
Figure 4 Scaling plots of swelling of PVI versus crosslinking density. The dashed line corresponds to the slope −0.60 (predicted by Flory's theory) and the solid lines to the linear fit of swelling (a) in methanol (slope −0.54 ± 0.05, correlation coefficient 0.94), (b) in ethanol (slope −0.46 ± 0.03, correlation coefficient 0.98), and (c) in water (slope −0.48 ± 0.05, correlation coefficient 0.94).

Since v_e scales with $C_T^{0.81} \times [BA]^{1.04}$, if S would depend on C_T and [BA] only through v_e, it should be expected that S would scale with $C_T^{-0.39} \times [BA]^{-0.50}$ for deionized water, with $C_T^{-0.37} \times [BA]^{-0.48}$ for ethanol and with $C_T^{-0.44} \times [BA]^{-0.56}$ for methanol. Never-
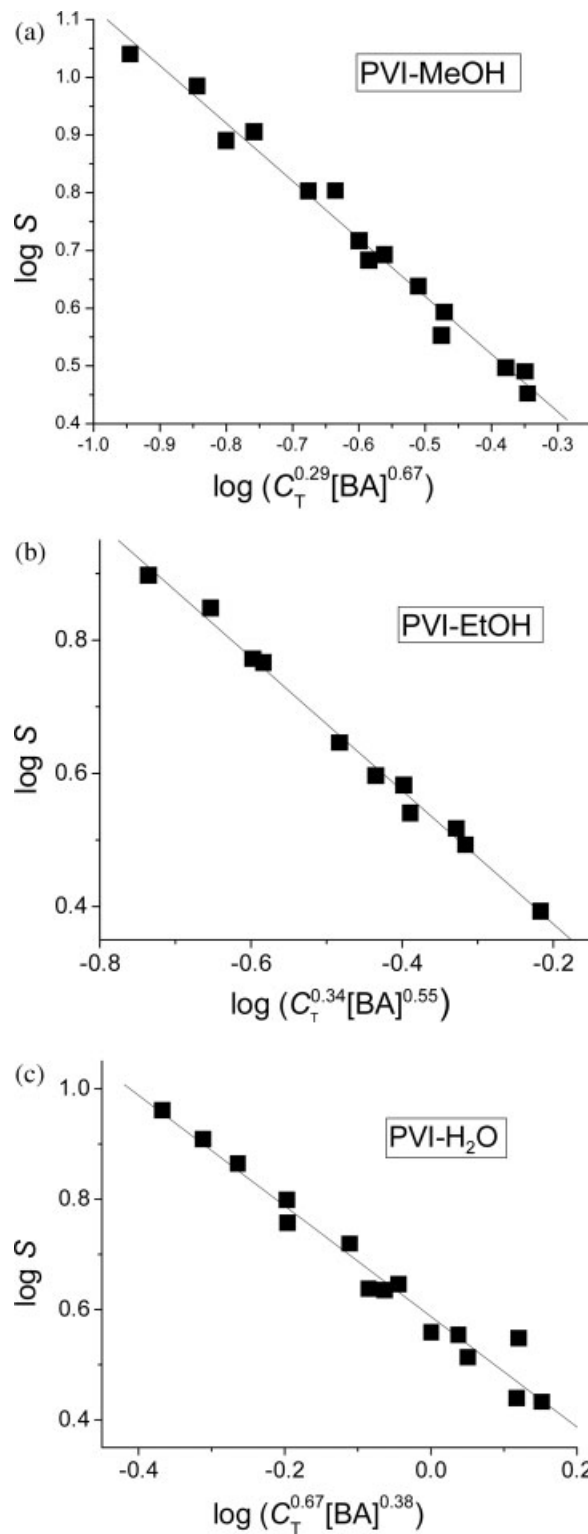

Figure 5 Swelling of PVI in methanol, ethanol, and water. Solid lines correspond to linear fits.

theless, the numbers shown in Table II are slightly but significantly different, indicating that S depends on feed not only through v_e but also through other parameters, likely through both v_{2r} and χ.

It is remarkable in Table II that the contribution of C_T and [BA] to S changes gradually increasing solvent goodness from water to methanol, and as long as the exponent of C_T decreases the [BA] one increases. Again, the role of C_T is difficult to understand. Contrary to predictions of the ideal polymer network model, S depends always inversely on C_T but the other two models included in Table II (PNPV and polymer network with entanglements) do neither predict the experimentally observed dependence of S on C_T and [BA] for any solvent. The model of polymer network with entanglements as unique topology different of an ideal network,[6] overestimates the contribution of C_T in any solvent although it is the largest at the smaller chain extensions (lower swelling, in water) in accordance with entanglements slippage considerations.[11] The contribution of [BA] is always in-between predictions of the model with entanglements and that with pendant vinyl's and the last model fails particularly in predicting the contribution of C_T in the good solvent, methanol. This suggests that in its largest part, PVI networks may be described with the PNPV model but different regions with other network defects and topologies contribute to swelling and their relative contribution depends on the goodness of the swelling solvent.

CONCLUSIONS

It was clearly stated that the stoichiometric ratio [BA]$/C_T$ does not represent the experimental cross-linking density of PVI hydrogels. By contrary, v_e correlates with $C_T \times$ [BA], which represents a coarse but acceptable approach of the model of PNPV to the experimental values. More precisely, for PVI, v_e scales with $C_T^{0.81} \times$ [BA]$^{1.04}$. The swelling degree of PVI in water, ethanol and methanol, scales with a power law of v_e which depends on solvent goodness, remaining slightly over the scaling exponent predicted by Flory ($S \sim v_e^{-0.6}$) or by de Gennes ($S \sim v_e^{-(3v-1)}$, with $v = 1/2$ for theta systems and $v = 3/5$ for good solvents). Finally, the scaling law of S with feed composition was found to be dependent on solvent and it seems to result not only from the dependence of v_e on C_T and [BA] but also from that of v_{2r} and χ.

This behavior is coherent with a polymer structure formed, predominantly, by a loose network well described by the model of pendant vinyl groups, and in a lesser portion, by domains with other defects and topologies. With regard to the role played by entanglements, models used seem to overestimate the experimental contribution of C_T to swelling due to entanglements.

References

1. Rivas, B. L.; Maturana, H.; Molina, M. J.; Gomez-Anton, M. R; Pierola, I. F. J Appl Polym Sci 1998, 67, 1109.
2. Molina, M. J.; Gomez-Anton, M. R.; Rivas, B. L.; Maturana, H.; Pierola, I. F. J Appl Polym Sci 2001, 79, 1467.
3. Bromberg, L.; Grosberg, A. Y.; Matsuo, E. S.; Suzuki, Y.; Tanaka, T. J Chem Phys 1997, 106, 2906.
4. Zhou, W. J.; Yao, K. J.; Kurth, M. J. J Appl Polym Sci 1997, 64, 1009.
5. Chen, J.; Zhao, Y. J Appl Polym Sci 2000, 75, 808.
6. Furukawa, H. J Mol Struct 2000, 554, 11.
7. Molina, M. J.; Pierola, I. F.; Gomez-Anton, M. R. Int J Polym Mater 2002, 51, 477.
8. Pastoriza, A.; Pacios, I. E.; Pierola, I. F. Polym Int 2005, 54, 1205.
9. De Gennes, P. G. Scaling Concepts in Polymer Physics; Cornell University Press: Ithaca, NY, 1979.
10. Flory, P. J. Principles of Polymer Chemistry; Cornell University Press: Ithaca, NY, 1953.
11. Chen, Z.; Cohen, C.; Escobedo, F. A. Macromolecules 2002, 35, 3296.
12. Oblukhov, S. P.; Rubinstein, M.; Colby, R. H. Macromolecules 1994, 27, 3191.
13. Rubinstein, M.; Colby, R. H. Macromolecules 1994, 27, 3184.
14. Baselga, J.; Fuentes, I. H.; Pierola, I. F.; Llorente, M. A. Macromolecules 1987, 20, 3060.
15. Xue, W.; Huglin, M. B.; Jones, T. G. J Eur Polym Mater 2005, 41, 239.
16. Gundogan, N.; Okay, O.; Oppermann, W. Macromol Chem Phys 2004, 205, 814.
17. Edwards, S. F. In Polymer Networks; Chompff, A., Newmann, S., Eds.; Plenum Press: New York, 1971.
18. Molina, M. J.; Gomez-Anton, M. R.; Pierola, I. F. Macromol Chem Phys 2075, 2002, 203.
19. Molina, M. J.; Gomez-Anton, M. R.; Pierola, I. F. J.; Polym Sci Part B: Polym Phys 2004, 42, 2294.
20. Isik, B.; Dogantekin, B. J Appl Polym Sci 2005, 96, 1783.
21. Bisht, H. S.; Wan, L.; Mao, G.; Oupicky, D. Polymer 2005, 46, 7945.
22. Pekel, N.; Salih, B.; Guven, O. J Biomater Sci Polym Ed 2005, 16, 253.
23. Fontanals, N.; Marce, R. M.; Galia, M.; Borrull, F. J.; Polym Sci Part A: Polym Chem 2004, 42, 2019.
24. Pacios, I. E.; Pierola, I. F. Macromolecules 2006, 39, 4120.
25. Pacios, I. E.; Pastoriza, A.; Pierola, I. F. Colloid Polym Sci, to appear.
26. Yoshinobu, M.; Morita, M.; Higuchi, M.; Sakata, I. J Appl Polym Sci 1994, 53, 1203.
27. Brannon-Peppas, L. In Absorbent Polymer Technology; Brannon-Peppas, L., Harland, R. S., Eds.; Elsevier: New York, 1990. Studies in Polymer Science, Vol. 8.
28. Espinasse, I.; Cassagnau, P.; Bert, M.; Michel, A. J Appl Polym Sci 1994, 54, 2083.
29. Orakdogen, N.; Okay, O. Eur Polym J 2006, 42, 955.
30. Horta, A.; Pastoriza, A. Eur Polym J 2005, 41, 2793.